# CONTROL OF MICRO-STRUCTURE EVOLUTION DURING HOT FORGING AND FORMING OF HIGH TEMPERATURE NICKEL BASED ALLOY LARGE MODULE SPUR GEARS BASED ON DEFORM 3-D

by

***Biyao YE, Zhenhong LI*, Yubao LU, Qi XIAO, Chaowei HU, Xiaoyu XIE, and Mengyang HU***

School of Materials Engineering, Nanjing Institute of Technology, Nanjing, China

Original scientific paper
https://doi.org/10.2298/TSCI250426229Y

*This paper presents the results of orthogonal simulation experiments conducted on the deformation temperature, friction factor, and deformation rate of process parameters for large modulus spur gears made of nickel based alloy GH738 with coarse grain size and non-uniform distribution, as well as other forming defects observed during hot forging and forming. These experiments were performed using DEFORM 3-D simulation software to optimize the combination of process parameters. During the experimental process, the evolution of the micro-structure and the impact of each factor on the average grain size and dynamic recrystallization volume fraction were observed. The influence level of each factor was then analyzed, and the optimal combination of process parameters was derived a deformation temperature of 1050 °C, a friction factor of 0.35, and a deformation rate of 55 mm/s. For the initial grain size of a 42 μm billet, after forming the gear tooth grain size uniformity, the dynamic recrystallization volume fraction reached 0.988, with an average grain size of 14.1 μm and a local grain size grade of 9. The forging and forming effect is optimal, with a relatively complete dynamic recrystallization reaction. The process parameter settings for the high temperature nickel based alloy gear precision molding provide a theoretical basis for improving the efficiency and quality of gear production.*

Keywords: *DEFORM 3-D, GH738, gear hot forging, orthogonal test, dynamic recrystallization*

## Introduction

Large modulus spur gears are essential transmission components widely used in aerospace, automotive manufacturing, and related fields, and their performance strongly affects the reliability and service life of high-end equipment [1]. Due to the difficulty of metal filling during die forging and the heavy loads borne by gear teeth in service, optimizing the forging process is crucial for improving manufacturing capability [2]. Current studies mainly focus on process optimization. Liu *et al.* [3] used finite element simulations to optimize forming parameters of cast AZ80A magnesium alloy spur bevel gears. Liu *et al.* [4] applied the 3-D numerical simulation program ABAQUS to study the influence of die structure on temperature forming. Shen *et al.* [5] simulated the warm forging upsetting process to identify defects and improve process design. Zhang *et al.* [6] used DEFROM 3-D simulation analyze temperature and deformation fields to address folding, high energy consumption, and low material utilization. However, the

* Corresponding author, e-mail: lizhenhongnj@163.com

aforementioned studies have primarily focused on optimizing the gear process solutions from the perspective of metal flow filling and macroscopic dimensions. There has been comparatively less research conducted on the optimization of the gear forming process with regard to micro-structure evolution control. While the existing forming process can effectively enhance the macro-scale qualification rate of gears produced, it is evident that the forging process, which involves prolonged heating and repeated deformation, introduces significant challenges. The heat treatment process for the surface and center of the gear entails disparate heating and cooling rates, resulting in substantial stress. Additionally, maintaining uniform temperature control and deformation across the gear is inherently difficult, increasing the likelihood of micro-structural defects such as coarse grains or reduced recrystallization volume fraction. These defects ultimately impair the mechanical properties of the gear, negatively impacting the overall quality of the gear production. For instance, Liu *et al.* [7] studied macro-segregation in hot-rolled steel to examine heat treatment deformation, yet comprehensive analysis of micro-structure evolution, especially grain size, is still lacking. Thus, a micro-structure-based control method is urgently needed to guide process parameter optimization and promote refined gear forging [8].

As the most widely used high temperature alloy, nickel is face-centered cubic and exhibits remarkable stability across a wide temperature range. It does not undergo isotropic transformation at room temperature or high temperatures, and its strong alloying ability allows for the addition of a variety of elements without the formation of harmful phases [9, 10]. Increasing demand for lighter and more integrated components in aerospace and new energy vehicles has accelerated the development of nickel based high temperature alloy processing technologies [11]. The GH738 alloy is widely used for aerospace transmission parts due to its oxidation resistance, high temperature strength, fatigue resistance, and good plasticity, making it suitable for forging process optimization. Therefore, studying the forging process of high temperature nickel based alloy large modulus spur gears is important for improving forming technology and enhancing gear mechanical properties.

In conclusion, this paper employs the finite element analysis software DEFORM [12] to investigate the micro-structure evolution of a high temperature nickel alloy with a large modulus during the spur gear forming process. The existing intrinsic model and dynamic recrystallization model serve as the foundation for simulation experiments, which employ an orthogonal experiment optimization design method and in-depth analysis of the change law of the micro-structure of nickel based alloys in gears. This approach also considers the optimization of the gear die forging forming process, with the objective of identifying the optimal combination of process parameters. The resulting parameters can then be reliably selected for production practice.

## Experimental design and numerical analysis

### *The GH738 intrinsic model selection and mold modelling*

The material utilized in this investigation is GH738 alloy, the primary components of which are delineated in tab. 1.

**Table 1. Chemical mass fractions [%)]of GH738 alloy**

| Chemical composition | Cr | C | Co | Mo | Al | Ti | P | Ni |
|---|---|---|---|---|---|---|---|---|
| GH738 | 20.0 | 0.08 | 14.0 | 4.0 | 1.0 | 3.0 | ≤0.015 | Tolerance |

In the existing research on material properties, Wang [13] obtained the true stress-strain curve of GH738 under different strain rates and temperature conditions through thermal compression test, and analyzed and calculated the related intrinsic model of the material. Based

on this foundation, a dynamic recrystallization model and constitutive equations were derived through a combination of the self-crystallization model in DEFORM software and the aforementioned experimental data:

$$\varepsilon_c = 0.851\varepsilon_p \tag{1}$$

$$\varepsilon_p = 3.53\cdot10^{-4} d_c^{0.54}\dot{\varepsilon}^{0.106}\left(\frac{49610}{RT}\right) \tag{2}$$

$$X_{\text{drex}} = 1-\exp\left[-0.693\left(\frac{\varepsilon-\varepsilon_c}{\varepsilon_{0.5}}\right)^{k_d}\right] \tag{3}$$

$$\varepsilon_{0.5} = 2.604\cdot10^{-19} d_0^{0.536}\dot{\varepsilon}^{-0.428}\exp\left(-\frac{14040}{RT}\right) \tag{4}$$

$$d_{\text{drex}} = 3.51\cdot10^{6} d_0^{0.197}\dot{\varepsilon}^{-0.105}\varepsilon^{-0.217}\exp\left(-\frac{145930}{RT}\right) \tag{5}$$

where $\varepsilon_c$ is the critical strain when dynamic recrystallization is on, $\varepsilon_p$ – the strain corresponding to the peak stress, $d_0$ [μm] – the original grain size, $\dot{\varepsilon}$ [$s^{-1}$] – the strain rate, R [$Jmol^{-1}K^{-1}$] – the gas constant, $T$ [K] – the thermodynamic temperature, $X_{drex}$ – the dynamic recrystallization percentage, $\varepsilon_{0.5}$ – the strain corresponding to a dynamic recrystallization percentage of 50%, $k_d$ – the Avrami exponent, the constant related to the material, which was determined to be 0.513 by a relevant calculation [14], and $d_{\text{drex}}$ – the dynamic recrystallization grain size.

The experimental parameter settings other than variables are shown in tab. 2.

**Table 2. Customized experimental variables**

| Mold materials | AISI-H-13 |
|---|---|
| Mold temperature [°C] | 300 |
| Ambient temperature [°C] | 20 |
| Heat transfer coefficient [$Wm^{-2}°C^{-1}$] | 11000 |
| Average grain size [μm] | 42 |
| Initial grain size [μm] | 42 |

Due to the lightweight design requirements in the aerospace field, gears must operate within more compact transmission systems while enduring higher stresses. Consequently, the typical large module range in such applications spans from 4-7. For this design experiment, gear parameters with a module of 5 are selected, as shown in tab. 3. In order to reduce the amount of calculation of the simulation experiment, this experiment uses 1/8 of the gear as a billet for the simulation experiment, and uses the UG body calculation function establish a billet model with the same volume, the gears and the mold modelling is shown in fig. 1.

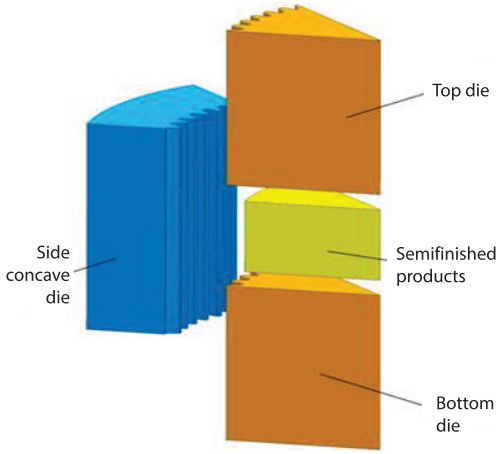


**Figure 1. The 3-D modelling of gears and dies**

**Table 3. Spur gear parameters**

| Gear parameters | Value |
|---|---|
| Modules [mm] | 5 |
| Tooth number | 48 |
| Pressure angle[ °] | 20 |
| Tooth width [mm] | 58 |

*Orthogonal test program design*

In order to ascertain the optimal selection of variables for the forging and forming processes of GH738, it is essential to consider the range of parameters and performance requirements associated with the production of gears. This necessitates an in-depth examination of the control of micro-structure evolution in GH738, which can be approached from three key perspectives: deformation temperature, friction factor, and deformation rate. In order to conduct the test, three factors and three levels were selected. The L9 (34) type orthogonal table was therefore, chosen for the design and calculation [15]. The orthogonal test factor level table is presented in tab. 4.

**Table 4. Table of experimental factor levels**

| Factor / Level | A<br>Deformation temperature [°C] | B<br>Friction factor | C<br>Deformation rate [mms$^{-1}$] |
|---|---|---|---|
| 1 | 1000 | 0.15 | 10 |
| 2 | 1050 | 0.25 | 55 |
| 3 | 1100 | 0.35 | 100 |

The orthogonal design structure matrix, as detailed in tab. 5 and comprising nine groups of process parameter combinations, was calculated and subjected to computer numerical simulation in DEFORM for each group of process parameter combinations in the table. The optimization target was the treatment of the tooth center position of the dynamic recrystallization grain size. The optimal process parameter combinations for the hot forging of GH738 large modulus spur gears were analyzed, and the average grain size and recrystallization volume component were integrated to assess the quality of the forgings. The results of the dynamic recrystallization grain size analysis, obtained following the finite element analysis of each group of process parameters, are presented in the tab. 5.

**Table 5. Orthogonal test protocol and results**

| Factor / Serial number | A<br>Deformation temperature [°C] | B<br>Friction factor | C<br>Deformation rate [mms$^{-1}$] | Pilot program | Dynamic recrystallization grain size, μm |
|---|---|---|---|---|---|
| 1 | 1000 | 0.15 | 10 | A1B1C1 | 26.6 |
| 2 | 1000 | 0.25 | 100 | A1B2C3 | 7.24 |
| 3 | 1000 | 0.35 | 55 | A1B3C2 | 5.62 |
| 4 | 1050 | 0.15 | 100 | A2B1C3 | 14.4 |
| 5 | 1050 | 0.25 | 55 | A2B2C2 | 14.6 |
| 6 | 1050 | 0.35 | 10 | A2B3C1 | 9.6 |
| 7 | 1100 | 0.15 | 55 | A3B1C2 | 15.1 |
| 8 | 1100 | 0.25 | 10 | A3B2C1 | 15.5 |
| 9 | 1100 | 0.35 | 100 | A3B3C3 | 17.8 |

## Results and discussion

*Results of orthogonal experiments*

The analytical method of orthogonal test can be used to achieve the analytical result data in tab. 6.

**Table 6. Analysis of orthogonal test results**

| Factor | Dynamic recrystallization grain size analysis | | | | | | |
|---|---|---|---|---|---|---|---|
| | $K_1$ | $K_2$ | $K_3$ | $k_1$ | $k_2$ | $k_3$ | R |
| Deformation temperature [°C] | 39.46 | 38.6 | 48.4 | 13.15 | 12.87 | 16.13 | 3.27 |
| Friction factor | 56.1 | 37.34 | 33.02 | 18.7 | 12.45 | 11.01 | 7.69 |
| Deformation rate [mms$^{-1}$] | 51.7 | 35.32 | 39.44 | 17.23 | 11.77 | 13.15 | 5.46 |

In the table, $K_i$ represents the sum of the results obtained from each group when the number of levels is $i$. Similarly, $k_i$ denotes the average of the results obtained from each group when the number of levels is $i$. Finally, $R$ represents the extreme deviation [16]. The analysis of the test results indicated that the primary and secondary relationships among the factors were friction factor > deformation rate > deformation temperature. Consequently, the optimal process parameter scheme was selected as $A_2B_3C_2$ on a preliminary basis.

According to the previous analysis, the optimal process parameter scheme analyzed in the orthogonal test is: deformation temperature 1050 °C, friction factor 0.35, deformation rate 55 mm/s. This set of parameters was set to DEFORM for computer numerical simulation and analysis of micro-structure and forging quality.

### *Simulation results of the best process parameter group*

Following the numerical simulation achieve the forging effect, as illustrated in fig. 2, the tooth was filled and the surface was smoothed. A small number of burrs were present at the end, but not on the working surface of the gear. These do not affect the overall quality of the forgings. To form this large module spur gear, a die forging assembly drawing was designed, as shown in fig. 3. During the die forging process, the billet is heated and deformed through extrusion. The upper die approaches the lower die at a set pressure and speed to close the die, driving the extrusion of key components 15 and 16. This causes the billet to contact the tooth-forming key part 4 during deformation. Continuous action gradually presses the material's mold side into the die, forming the tooth profile. Upon completion of forging, the billet's side surface achieves full conformity with the tooth profile of component 4, resulting in the complete formation of the tooth profile.

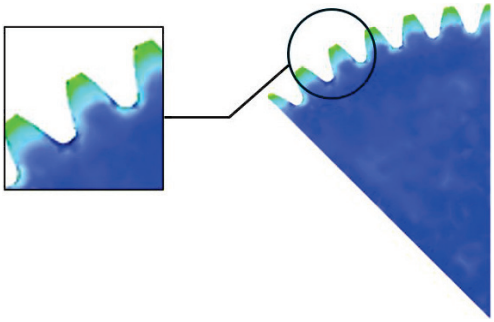

**Figure 2. The $A_2B_3C_2$ forging effect diagram**

As illustrated in fig. 4, the billet exhibits minimal deformation, with a correspondingly low equivalent strain. However, an increase in the equivalent strain can facilitate the intensification of material grain deformation, leading to enhanced energy storage, elevated dislocation density, and ultimately, reaching the critical strain point, triggering dynamic recrystallization. However, the equivalent strain of the central portion of the billet does not reach the critical strain required to initiate dynamic recrystallization. Consequently, the volume of dynamic recrystallization in this region is minimal, and no discernible dynamic recrystallization phenomena are observed. In contrast, the outer portion of the billet, which forms the tooth-like structure, is subjected to significant stress and generates a large strain, reaching approximately 1.61. This

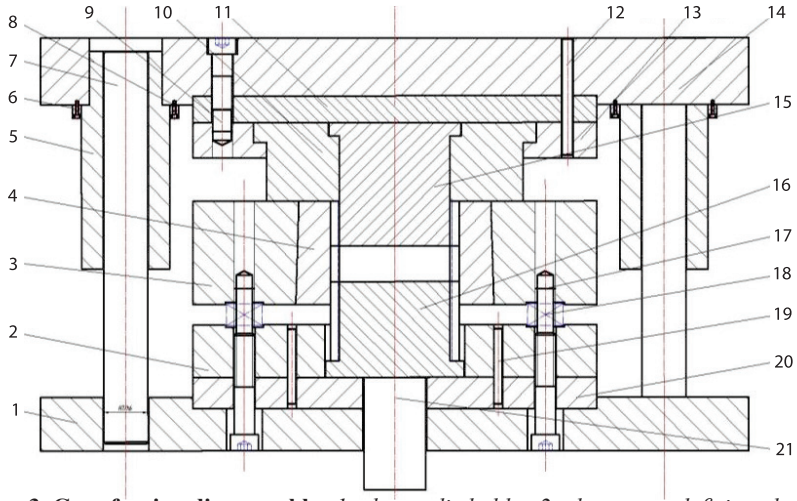


**Figure 3. Gear forging die assembly;** *1 – lower die holder, 2 – lower punch fixing plate, 3 – concave die outer ring, 4 – concave die inner ring, 5 – guide sleeve, 6 – fixing flange, 7 – guide pillar, 8, 9, and 17 – hexagon socket head cap screws, 10 –upper punch sleeve, 11 – upper punch plate, 12 and 19 – pin, 13 – upper punch fixing plate, 14 – upper die holder, 15 – upper punc, 16 – lower punch, 18 – spring, 20 – lower punch plate, and 21 – roof bar*

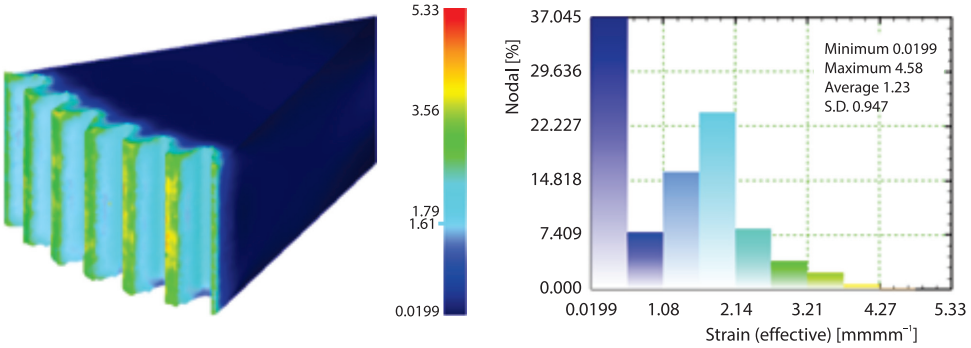


**Figure 4. Equivalent strain distribution of forgings**

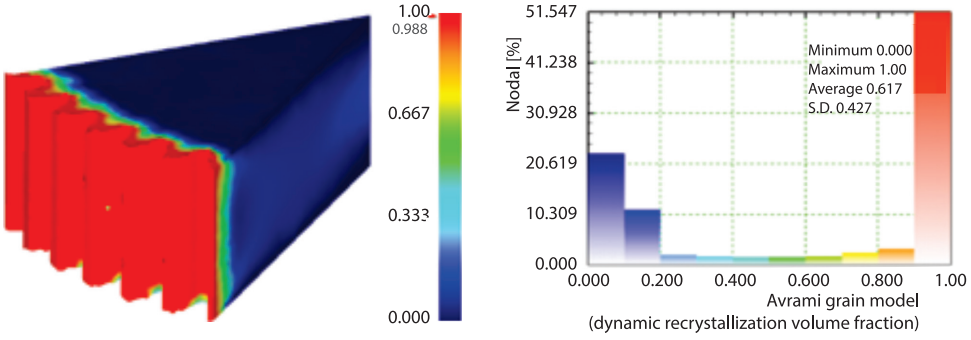


**Figure 5. Dynamic recrystallization volume fraction distribution of forgings**

environment is more conducive to the occurrence of dynamic recrystallization. The upper portion of the tooth, in particular, experiences significant strain due to the one-way compression of the single-acting die. This leads to a more complete dynamic recrystallization process and the formation of a recrystallization volume fraction distribution, as illustrated in fig. 5. The maximum dynamic recrystallization volume fraction reaches 1. The dynamic recrystallization volume fraction at the center of the tooth surface reaches 0.988, and the average dynamic recrystallization volume fraction is 0.617. These observations indicate that dynamic recrystallization behaviors are concentrated in the gear tooth.

*Analysis of the effect of deformation temperature*

Figure 6 illustrates the mean grain size distribution at three temperature levels when the optimal process parameter sets, $A_1B_3C_2$, $A_2B_3C_2$, $A_3B_3C_2$, correspond to a constant friction factor and deformation rate. The grain sizes of the centroid of the tooth at 1000 °C, 1050 °C, and 1100 °C are 5.88 μm, 14.1 μm, and 15.5 μm, respectively. The overall pattern is that, the higher the temperature, the faster the equivalent strain and equivalent force of the centroid of the tooth gradually decrease, resulting in an upward trend in the overall grain size change. Overall, the higher the temperature is, the equivalent strain and the equivalent force at the center point of the tooth shape gradually decrease, and the growth of the recrystallized grains accelerates after shaping, resulting in an upward trend in the overall change of grain size. For gear tooth, with the increase of temperature, the minimum value of dynamic recrystallization volume fraction and recrystallization volume fraction increases, that is, the increase of the deformation temperature will make the recrystallization more complete, but too high a temperature will also lead to grain growth after recrystallization, so it is necessary to play the role of the temperature on the maximum enhancement of the volume fraction of recrystallization, to reduce the growth of grains due to the increase in temperature on the overall micro-structure of the organization. Therefore, it is necessary to minimize the effect of grain growth on the overall micro-structure due to temperature increase while maximizing the effect of temperature on recrystallization volume fraction. Because of the small difference between the temperature variables in this experiment, the temperature has the least influence on the micro-structure evolution compared to the other two factors.

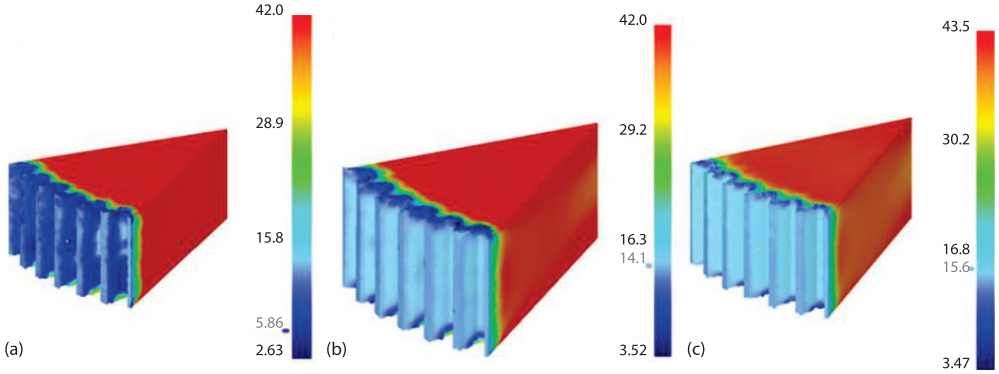


**Figure 6. Average grain size size [μm] at different temperatures: (a) 1000 °C, (b) 1050 °C, and (c) 1100 °C**

While the average grain size of the gear tooth is the smallest at 1000 °C in this experiment, the distribution of the grain size of the tooth is not uniform, as evidenced by the distribution of the color blocks in the cloud diagram. While the average grain size of the upper portion of the tooth is

larger, reaching approximately 15 μm, the average grain size of the majority of the middle section is smaller, at 5.88 μm. This discrepancy between the upper and middle sections results in reduced strength and inferior molding quality. Furthermore, the dynamic recrystallization volume fraction of the gear tooth at 1000 °C is 0.968. Following an increase in temperature, the value is slightly reduced in both experimental groups. However, it is notable that all samples reach a value of 0.9 or above. The experimental group subjected to a higher temperature displays a more uniform distribution of grain organization and a higher tooth strength than the experimental group subjected to a lower temperature. This is despite the average grain size being larger. Based on the simulation results, it can be posited that the dynamic recrystallization grain size and recrystallization volume fraction have reached a relatively reasonable equilibrium state at 1050 °C.

### *Analysis of the influence law of friction factor*

The friction factor modifies the contact conditions between the mold and the billet, which directly alters the level of friction between the material and the mold. High friction restricts the uniform flow of the material in the mold, resulting in stress concentration and uneven deformation. The high temperature alloy exhibits a high flow stress, rendering it particularly susceptible to alterations in the friction factor during precision forging. When the friction is excessive, the flow stress is amplified, impeding the plastic flow of the material and hindering the full development of deformation. Furthermore, the hot forging forming process generates frictional heat, which affects the evolution of the micro-structure. In light of the aforementioned considerations, it can be concluded that the friction factor exerts the most significant influence on micro-structure evolution in the context of this experiment. The simulation results indicate that the optimal friction factor value is 0.35.

Figures 7 and 8 illustrate the equivalent strain and equivalent force changes for the $A_2B_1C_2$, $A_2B_2C_2$, and $A_2B_3C_2$ groups, which exhibit disparate friction factors. The overall change rule of equivalent strain is that with an increase in the friction factor, its value exhibits a slight upward trend. As the friction factor rises from 0.15-0.25, the equivalent strain of the gear tooth increases from 1.48-1.6. This indicates that the value interval is more appropriate, the relative sliding between the material and the mold is more balanced, and the appropriate increase of the friction factor promotes the uniform flow of the material, resulting in a more uniform deformation. As the friction factor continues to increase to 0.35, the peak equivalent strain in the tooth area increases only slightly to 1.62. However, the distribution of equivalent strain on the tooth becomes more uniform. Given that the molding is a unidirectional closed die forging, the metal flow resistance in the downward and top directions is minimal when the friction factor is low. This results in the filling of the tooth shape occurring from the bottom to the top, with the deformation not being uniform along the tooth height direction. As the friction factor increases, the downward flow of metal becomes more challenging. However, the filling of the entire tooth height simultaneously improves, resulting in a more uniform overall deformation. Consequently, the corresponding equivalent force is reduced, and the performance of the friction factor exhibits an inverse correlation with the increase in the friction factor. When the friction factor is 0.15, the equivalent force of the gear tooth is 907 MPa. Upon increasing the friction factor to 0.25 and 0.35, the equivalent force decreases to 404 MPa and 346 MPa, respectively. Additionally, the average grain size and the dynamic recrystallization volume fraction of each group can be observed when the friction factor is 0. The dynamic recrystallization volume fraction is larger and the average grain size is smaller as a result of the increase in friction factor. This is due to the fact that under these conditions, the material undergoes sufficient plastic deformation with a high equivalent strain and maintains a low stress level with a moderate equivalent stress.

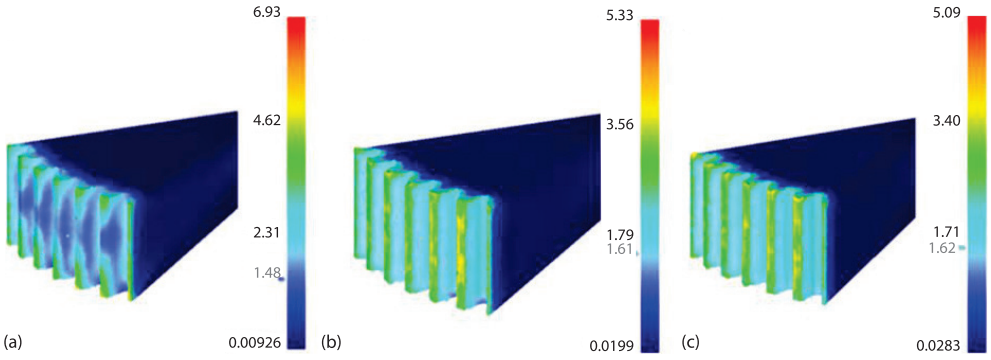


**Figure 7. Equivalent strain for different friction factors: (a) 0.15, (b) 0.25, and (c) 0.35**

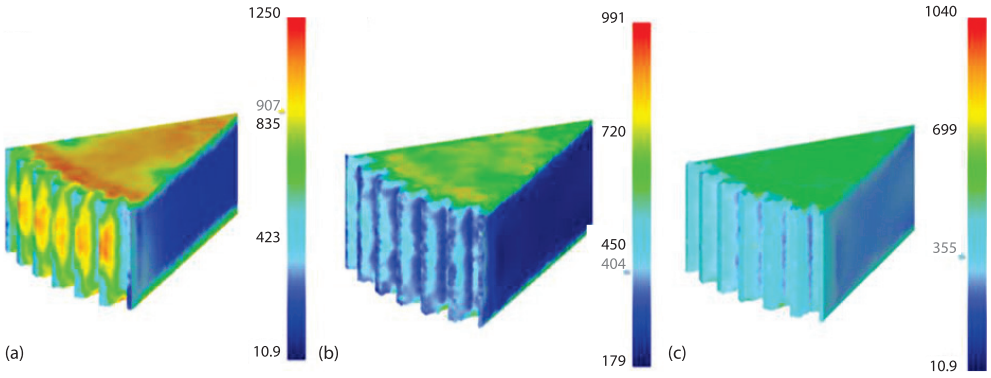


**Figure 8. Equivalent force for different friction factors [MPa]; (a) 0.15, (b) 0.25, and (c) 0.35**

### *Analysis of the effect of deformation rate*

The influence of deformation rate on micro-structure evolution is primarily mediated by varying deformation temperatures across different deformation rates. As deformation rate increases, the average grain size tends to diminish. This phenomenon can be attributed to the fact that an increase in deformation rate results in the inability of the alloy to release heat within a short period of time. This leads to an elevated local temperature within the alloy, which in turn promotes the occurrence of dynamic recrystallization in the region. Additionally, the elevated local temperature within the alloy facilitates alloy dynamic recrystallization and grain growth. Consequently, the alteration of deformation rate essentially entails a modification of temperature conditions, thereby influencing the evolution of the micro-structure during the hot forging and forming process. However, when the deformation rate is excessively high, the equivalent strain accumulates rapidly. Deformation rates that are too fast do not allow for sufficient time for dynamic recrystallization, which results in grains in some areas not being refined in time. This can lead to the formation of work-hardening, as well as the emergence of residual stresses and an inhomogeneous grain structure within the material. The analysis of the aforementioned study, coupled with the considerable variability observed in the deformation rate during experimentation, indicates that its impact on micro-structure evolution is more pronounced than that of deformation temperature but less pronounced than that of friction factor. Accordingly, the optimal deformation rate is deemed to be 55 mm/s, as substantiated by the simulation validation results.

### *Metallographic analysis of optimal process parameter combinations*

To verify the micro-structural effects of gears forged under the optimal process parameters identified in this paper, and to analyze their evolution patterns further, a metallographic observation was conducted on the critical location of the gear tooth core, as shown in fig. 9. From an overall micro-structural perspective, the metallographic image reveals a uniform grain structure in the tooth core with small grain sizes and no obvious defects, such as coarse grains or segregation. Further data analysis yielded an average grain size of approximately 14.3 μm, which closely matches the result of 14.1 μm obtained through numerical simulation. This indicates that the dynamic recrystallisation reaction was sufficiently developed and closely aligned with the simulation predictions. Thus, metallographic observation confirms that the optimal combination of process parameters effectively controls the micro-structural evolution of the GH738 alloy and that the simulation results obtained in this study are highly reliable.

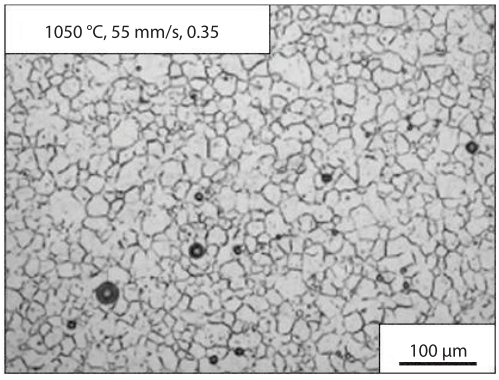


**Figure 9. Metallographic micro-structure of gear tooth core under optimal process parameters**

## Conclusions

The objective of this study is to enhance the micro-structure of the GH738 high temperature nickel based alloy large modulus spur gear hot forging by optimizing the deformation temperature, friction factor, deformation rate, and other hot forging process parameters. To achieve this, an orthogonal optimization method was employed to optimize the forging process design.

- The primary and secondary relationships affecting the micro-structure grain size of the GH738 high temperature nickel based alloy in the hot forging of large module spur gears can be attributed to the following factors in descending order of importance: friction factor, deformation rate, and deformation temperature.
- The optimal combination of process parameters for the GH738 high temperature nickel based alloy in the hot forging of large module spur gears is a deformation temperature of 1050 °C, a friction factor of 0.35, and a deformation rate of 55 mm/s.
- The optimal combination of process parameters allows for the production of a forging with complete filling and uniform grain size. The average grain size is 14.1 μm, and the recrystallized volume fraction of the tooth of the forging reaches 0.988, indicating that the local grain size reaches grade 9.

The results of this study will provide a theoretical basis for the improvement of the process of hot forging of gears. This, in turn, will be conducive to the development of the fine closed die forging process and the innovation of the observation angle. Furthermore, it will contribute to the production of large modulus spur gears.

## Acknowledgment

This research was carried out with the financial support of the Practical Innovation Training Program for College Students in Jiangsu Province of China (202311276012Z).

## References

[1] Hua, L., *et al*., Research and Application of Theory Technology and Equipment on Gear Precision Plastic Forming, *Journal of Plasticity Engineering*, *31* (2024), 4, pp. 56-73
[2] Lang, X., Fang, Y. S., Research on Manufacturing Technology of Gear Forgings, *Valve*, *31* (2024), 1, pp. 101-104
[3] Liu, J. J., *et al.*, Hot Forging Process Optimization of Magnesium AlloyGear Based on DEFORM-3D, *Journal of Taiyuan University of Technology*, *44* (2023), 4, pp. 334-338
[4] Liu, F. G., Warm Forging Process and Die Optimization Design of Large Modulus Spur Gear Based on ABAQUS Simulation Software, *Hot Working Technolog*, *47* (2018), 11, pp. 176-178
[5] Shen, Y. H., *et al*., Optimization of Warm Forging Forming Technology of Cylinder Spur Gear with Big Modulus, *Hot Working Technology*, *43* (2014), 3, pp. 137-140
[6] Zhang, H., *et al*., Research on the Shunting Precision Forging of Ribbed Plate Gear Blank Based on DEFORM-3D Finite Element Analysis Under the Framework of New Engineering, *Journal of Physics: Conference Series*, *1302* (2019), 042029
[7] Liu, S., *et al*., Finite Element Analysis on Shape Deformation of the Macro-Structure Region during Hot-Rolling Process for Gear Steel FAS3420H and Its Modification, *Materialwissenschaft und Werkstofftechnik*, *52* (2021), 7, pp. 792-804
[8] Zhang, X. F., Research on Optimization of Manu-facturing Process for Mechanical Gear Forgings Based on Intelligent Manufacturing Technology, *Modern Manufacturing Technology and Equipment*, *60* (2024), 6, pp. 128-130
[9] Gai, Y. C., *et al*., Solidfication Segregation Behavior and Homogenization Heat Treatment of GH4151 Alloy, *Rare Metal Materials and Engineering*, *53* (2024), 1, pp. 159-168
[10] Wang, C., *et al*., Influence of Cold Deformation and Heat Treatment on Micro-Structure and Properties of GH738 Nickel-Based Alloy, *Heat Treatment of Met-als*, *50* (2025), 3, pp. 25-31
[11] Wu, Y., *et al*., Progress in Research and Applications of Additively Manufactured Nickel-Based Superalloy in Aero-Engines and Gas Turbines, *Journal of Aeronautical Materials*, *44* (2024), 1, pp. 31-45
[12] Chen, B. S., Lu, Y. J., Analysis and Experimental Verification of Gear Billet Precision Forging Process Based on Deform-3D, *Forging & Stamp-ing Technology*, *48* (2023), 12, pp. 18-24
[13] Wang, X. K., Numerical Simulation Research on Hot Forging Process of GH738 Superalloy Bolt, M. Sc. thesis, Harbin Institute of Technology, Harbin, China, 2021
[14] Guo, J., *et al*., Dynamic Recrystallization Model Analysis of New Type High Quality GH738 Alloy during Its Hot Deformation Processes, *Journal of Mechanical Engineering*, *58* (2022), 10, pp. 59-67
[15] Yin, T. T., Research on Warm Closed-Die Forging Process of Straight Bevel Gear Based on DEFORM-3D, *Journal of Kaifeng University*, *37* (2023), 1, pp. 67-70
[16] Chen, K., *Design and Analysis of Experiments*: Tsinghua University Press, Beijing, China, 2005

Paper submitted: April 4, 2025
Paper revised: November 25, 2025
Paper accepted: November 30, 2025

2026 Published by the Vinča Institute of Nuclear Sciences, Belgrade, Serbia.
This is an open access article distributed under the CC BY 4.0 terms and conditions.